IU ST
Iran University of Science and Technology

Iranian Journal of Electrical and Electronic Engineering

Journal Homepage: ijeee.iust.ac.ir

Comparative Analysis of Polar Coded F-OFDM and UFMC 5G NR Waveforms

Smita Jolania*(C.A), Ravi Sindal**

Abstract: Fifth Generation-New Radio (5G-NR) is an advanced air interface defined to fulfil diverse services with ubiquitous coverage in next generation Wireless networks. The waveform is the crucial part of air interface that must have good spectral confinement and low peak-to-average power ratio (PAPR). Orthogonal Frequency Division Multiplexing (OFDM) is a widely used air interface in Fourth Generation Long Term Evolution (4G-LTE) system. But OFDM suffers from high PAPR, Carrier Frequency offset (CFO), and loss of spectral efficiency due to insertion of cyclic prefix. So, the high dense networks with heterogeneous traffic in the 5G requires new multicarrier waveform. In the proposed work, waveforms based on sub-band filtering are considered due to more flexibility and shorter filter length as compared to the sub-carrier-based filtering waveforms. Two major 5G waveform candidates Filtered-Orthogonal Frequency Division Multiplexing (F-OFDM) and Universal Frequency Division Multiplexing (UFMC) are proposed in the system design. Channel coding is the inherent part of air interface for enhancing the error performance. New error correcting channel codes introduced in NR to support variable information block length and flexible codeword size. The capacity achieving Polar codes is the highlight of this paper adopted for control channels. 5G NR air interface using new modulation waveform along with the polar coding can be an effective way to enhance error performance. This paper presents comparative analysis of comprehensive systems Polar coded F-OFDM (PC-F-OFDM) and Polar coded UFMC (PC-UFMC) in massive MIMO scenario. Simulation results indicate that the proposed PC-F-OFDM systems significantly outperform the PC-UFMC systems in AWGN channel. But in massive MIMO setup BER performance of PC-UFMC is better than PC-F-OFDM system.

Keywords: New Radio, F-OFDM, UFMC, Polar Codes, Massive MIMO

1 Introduction

THE major trends observed in 5G are virtual reality and augmented reality applications, machine-to-machine (M2M) communication, high traffic density, Connectivity on moving platforms, mobile high-definition multimedia, Inter of Things (IoT) etc. [1]. The future wireless network is targeted to meet the diversified data requirements such as high data rate (20 Giga bits per second), massive device density (106 devices/Km2), and ultra-low latency (less than 1ms) for applications such as Driverless cars, enhanced mobile cloud services, real-time traffic control optimization, smart grid, e-health, high-speed trains, immersive video conferencing etc. [2]. The physical layer of 5G must be efficiently designed to multiplex the above-mentioned services with optimization of quality of service. The waveform design for the 5G air interface has the potential to meet these diversified requirements [3]. Orthogonal Frequency Division Multiplexing (OFDM) is one of the most prominent waveform candidates in Fourth Generation-Long Term Evolution (4G-LTE) due to

Iranian Journal of Electrical & Electronic Engineering, 2024.
Paper first received 6 December 2023 and accepted 13 March 2024
* The author is with the Department of Electronics and Communication Engineering, Devi Ahilya Vishwavidyalaya, Indore, India
E-mail: sprajapati2911@gmail.com

** The author is with the Department of Electronics and Communication Engineering, Devi Ahilya University, Indore, India
E-mails: rsindal@ietdavv.edu.in
Corresponding Author: Smita Jolania.

efficient spectrum utilization, combating inter-carrier interference (ICI), and Inter symbol interference (ISI) [4]. Critical issues related to the OFDM technique are its high out of band emissions (OOBE) and Peak to Average power ratio (PAPR). If the orthogonality is lost, ISI or ICI may become severe. Also, it has limited flexibility to adapt for various channel conditions [5].

For better spectral confinement and efficient spectral utilization, filtering techniques applied along with multi carrier modulation techniques. Major 5G waveform candidates in race are Filter Bank Multi Carrier (FBMC) [5], Generalized Frequency Division Multiplexing (GFDM) [6], UFMC [7], and F-OFDM [8]. A comprehensive analysis of these waveforms discussed in [9], concludes that a particular waveform cannot fulfil heterogeneous requirements of 5G. Broadly these waveforms are classified into two major categories: Subcarrier based filtering and sub-band-based filtering. FBMC and GFDM are techniques based on subcarrier wise filtering that makes the system robust against ISI [10]. But they require a new transceiver design, and there is no backward compatibility with 4G-LTE [11]. Sub-band-wise filtering is considered better than subcarrier-wise filtering in terms of flexibility and shorter filter length and most suitable for low latency applications. In sub-band filtering techniques, the total available bandwidth partitioned into sub-bands and fixed frequency-domain filtering is performed [12]. UFMC and F-OFDM are the two major 5G waveforms based on sub-band filtering and are the major highlight of the paper.

Channel coding applied at the physical layer to minimize the impact of Rayleigh channel and to reduce the error probability. In 5G-NR air interface, two major channel coding techniques proposed are: low-density parity-check (LDPC) codes and Polar codes [13]. The LDPC codes applied for user data and polar codes for control information. Polar codes are capacity-achieving codes with low computational complexities [14]. The polar codes implemented in the system design provide full flexibility with exceptionally superior performance in any code length and code rate [15]. Sharma, Arti et. al. in [16], proposed that 5G polar control codes be designed particularly for short block length to resolve the latency issue needed in Ultra Reliable Low Latency Communication (URLLC). The performance of PC-F-OFDM over additive white Gaussian noise (AWGN) channel shown in [17] and comparison with PC-OFDM presented. It clearly proves that PC-F-OFDM system outperforms PC-OFDM in terms of bit error rate (BER). PC-UFMC system has been analyzed, designed, and simulated in this research work.

5G NR air interface along with the Massive Multiple input multiple output (MIMO) technology can be an effective way to meet the enormous traffic demands of 5G networks [18]. Massive MIMO implements larger antenna arrays usually hundred or more antennas at the base station (referred to as gNodeB (gNB) in 5G NR terminology) to improve the network capacity and throughput [19]. The concept of massive MIMO was introduced by T.L. Marzetta in [20], who concluded that asymptotically as the number of antennas at gNB$\rightarrow \infty$, the system processing gain proportionally increases or tends to infinity.

The remaining section of this paper is organized as follows: In section II the waveform design aspects and the transmitter for F-OFDM and UFMC are presented with mathematical models of filters applied. Section III gives an overview of polar encoding and decoding. Then, the proposed PC-FOFDM and PC-UFMC system with massive MIMO scenario over Rayleigh channel presented in Section IV. In section V simulation parameters and the results are presented. Lastly the comparative analysis concluded in section VI. In this paper, a comparison of Bit error rate (BER) performance of polar coded waveform techniques F-OFDM and UFMC with massive MIMO antenna array evaluated.

2 Modulation Technique

The waveforms considered in the paper are based on sub-band filtering. Sub-band wise filtering refers to a band divided into multiple sub-bands. The sub-bands can have a different bandwidth. Each sub-band is comprising of multiple subcarriers and the inter subcarrier spacing can differ with each sub-band. Therefore, these waveforms provide both sub-band and subcarrier flexibility to facilitate diverse services of 5G. The following sub-sections describe the F-OFDM and UFMC waveform transmitter blocks.

2.1 Filtered OFDM (F-OFDM)

The best Zhang et. Al. in [8], depicted that the F-OFDM is the most flexible waveform for 5G for overcoming the drawbacks of OFDM. F-OFDM is MIMO-friendly and flexible dynamic spectrum sharing. In this waveform, customized numerology of different time-frequency grid helps to meet certain channel conditions and applications [21]. An analytical comparison of 5G waveform candidates in terms of spectral efficiency, robustness, energy efficiency, and numerical complexity shown in [11], proved that F-OFDM is the most adaptable waveform for 5G at the cost of increased complexity. The bandwidth in F-OFDM split into separate sub-bands in the time domain and modulated using OFDM.

Let us consider an F-OFDM system containing P subcarriers divided into B sub-bands in the time domain with each sub-band transmitting M contiguous subcarriers, i.e., $P = M \cdot B$. Fig. 1 depicts the transmitter

scheme. Let the generated symbols transmitted in each sub-band represented in vector form as equation (1):

$$S = [s_1, s_2, s_3, \dots, s_B]_{P\times 1} \quad (1)$$

The signal transmitted in the bth sub-band represented as s_(b) as equation (2):

$$s_b = [s_b(1), s_b(2), \dots, s_b(M)]^T_{M\times 1} \quad (2)$$

During each OFDM symbol period, the transmitter obtains length-N IFFT of M QAM modulated data symbols together with a CP [22]. LCP presents the CP size. Therefore F-OFDM signal created by B OFDM sub-symbols with a length of M + LCP [23].

The F-OFDM signal obtained by passing the signal through an appropriately designed spectrum shaping filter h(t) of the length L on each sub-band b. The length of filter should be set to half of the OFDM symbol. Windowed sinc functions used in the filtering operation. The desirable filter properties are Passband needs to be uniform over the range of subcarriers, the size of the guard bands needs to decreased, and good stop-band attenuation, with shorter side lobes [24]. In the system design a low pass Finite Impulse Response (FIR) filter designed by truncating the sinc function by a Hanning window. The designed low-pass filter is obtained by applying a window w(t) on the impulse response of Sinc filter, i.e.

$$h_B(t) = sinc_B(t) \cdot w(t) \quad (3)$$

The window has smooth transitions to zero on both ends so that it avoids abrupt jumps at the beginning and end of the truncated filter, and hence, avoids the frequency leakage in the truncated filter [25]. Generalized expression for the applied window $w(t)$ given by:

$$w(t) = \begin{cases} 0.5\left[1+\cos\left(\frac{2\pi t}{L}\right)\right]^{\alpha}, & |t| \le \frac{L}{2} \\ 0, \quad \Delta & |t| > \frac{L}{2} \end{cases} \quad (4)$$

where α is the roll-off factor used to control the shape of the window, and L is the filter length. α=1, it becomes a Hann window.

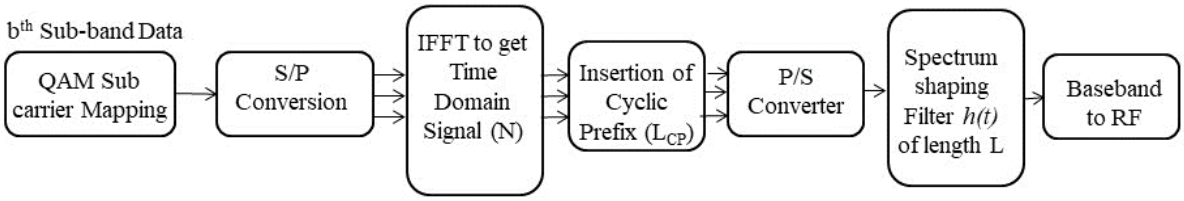

Fig. 1 F-OFDM Transmitter

2.2 Universal Filtered Multicarrier (UFMC)

Like F-OFDM, in UFMC modulation, the available bandwidth split into B sub-bands. Here, sub-band filtering is applied in frequency domain to reduce OOBE. Due to fine frequency filtration, shorter filter length and compatibility with MIMO, UFMC is the most suitable waveform for short burst communication in 5G. QAM symbol mapping applied for ith sub-band data stream. The complex frequency domain QAM symbols [s1, s2, s3, …. sob] transformed to time-domain by N-IFFT module with IFFT matrix [Vi]. Then, sub-band filtering was done by prototype Dolph- Chebyshev filter of length 'L' whose impulse response matrix is Fi [26]. The complete UFMC modulation process is shown in fig 2.

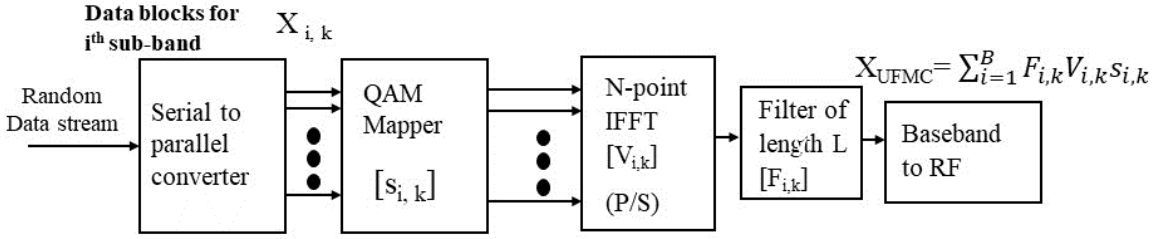

Fig. 2 UFMC Transmitter

In Dolph Chebyshev filters width of the main lobe is minimized for a given α side lobe attenuation and the mathematical expression of Chebyshev window is shown in equation (5) [27].

$$f = \frac{\cos\left\{N.cos^{-1}\left[\beta\cos\left(\frac{\pi k}{N}\right)\right]\right\}}{\cos[N\,cosh^{-1}(\beta)]} \quad (5)$$

Where N denotes for IFFT points, k=0, 1…, M-1, $\beta = \cosh\left\{\frac{1}{N}cosh^{-1}(10^{\alpha})\right\}$, α= (2,3,4). The 'α' parameters adjust the side lobe levels by the expression Side lobe level in dB=−20α. The UFMC waveform achieves better spectrum utilization than F-OFDM as UFMC has no CP. The time domain and frequency domain characteristics of filters used in F-OFDM and UFMC used are shown in fig. 3. Fig.4, and Fig. 5.

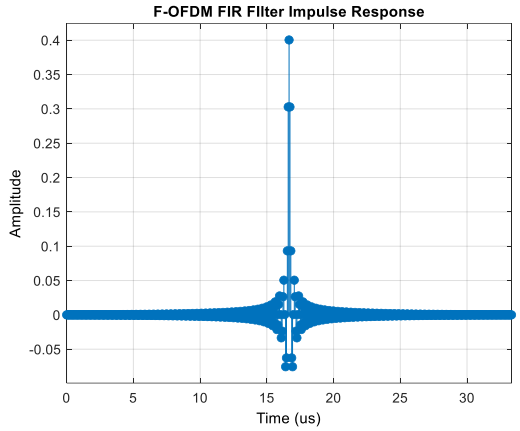

Fig. 3 Filter Impulse Response used in F-OFDM with filter length L=513

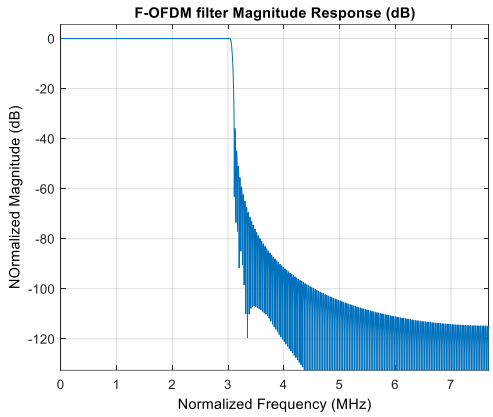

Fig. 4 Filter Frequency response used in F-OFDM with filter length L=513

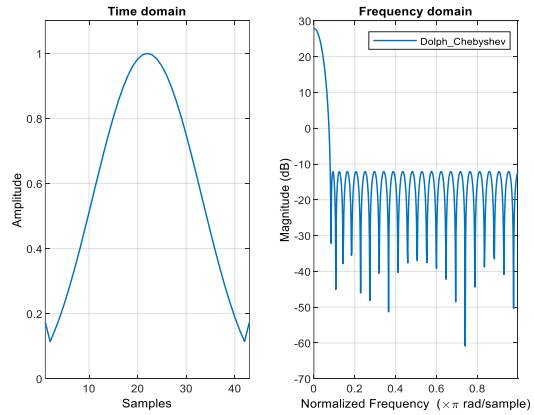

Fig. 5 Filter characteristics used in UFMC with filter length L=43 and α=40

3 Channel Coding Technique

3.1 Polar Coding

Polar codes have a unique structure able to attain the channel capacity of memory less, binary-input, output-symmetric (MBIOS) channels. In 5G NR, Polar codes are adopted as a channel coding applied for control channels. A (N, K) polar code where N is encoded bits and K is information bits, is defined by its channel transformation matrix $G_N = G_2^{\otimes n}$. It is the n^{th} Kronecker power of the polarizing matrix G_2 represented by equation (6) with $n=\log_2 N$ [28].

$$G_2 = \begin{bmatrix} 1 & 0 \\ 1 & 1 \end{bmatrix} \quad (6)$$

For MBIOS channels, the index 'i' set I ∈ {1, 2, · · ·, N} is called information set and the value of these fixed positions are called frozen bits (F). An auxiliary input vector $u = [u_0, u_1, \ldots, u_{N-1}]$ of length N is generated by assigning $u_i = 0$ if i ∈ F and storing the information bits in the remaining entries. Code word $x = [x_0, x_1, \ldots, x_{N-1}]$ is then calculated as equation (7):

$$x = u \cdot G_N \quad (7)$$

The recursive structure of G_N allows reducing the encoding complexity. W be the Binary Erasure Channel (BEC) implement the transform that polarizes the output x.

$$y = x.\ W \quad (8)$$

3.2 Polar Decoding

There are a variety of algorithms for decoding Polar encoded messages. Arikan proposed the Successive Cancellation (SC) technique in [29] as one of the first decoding algorithms. In SC, at every decoding stage, it determines whether to move forward along a current path or move backward to find a new path with higher reliability. Every node at stage receives soft information in the form of logarithmic likelihood ratios (LLRs) from its parent node and returns the hard decision. The depth of the tree is first investigated, with emphasis on the left branches. SC decoding is not suitable for short block lengths. Successive Cancellation List (SCL) Decoding is employed to get around this issue. Many possible pathways will be gathered and listed during the SCL decoding process. One path is chosen from the decoding paths in the SC decoder, but L_{max} of the best decoding paths are activated and maintained simultaneously in the SCL decoder [30]. SCL becomes more efficient as the list size grows, but its implementation becomes more difficult. Let $\hat{u}_i$ be estimate of Source block, the bits $\hat{u}_i$ are determined successively with index i from 1 to N in the following way:

$$L = \hat{u}_i^{(i-1)}(1), \ldots . \hat{u}_i^{(i-1)}(L_{max}) \quad (9)$$

L distinct decoding paths after the $(i-1)^{th}$ bit has been decoded. For every path $t \in \{1, \ldots, L_{max}\}$, there are two choices for $\hat{u}_i(t)$. Out of the resulting $2L_{max}$ paths, the L_{max} paths with the highest metric are preserved. When bit N is reached, the path with the highest metric is set as the decoded codeword [31].

4 System Model

Comprehensive block diagram of system for transmitter and receiver section applied for simulation using PC-F-OFDM and PC-UFMC with massive MIMO scenario over Rayleigh channel has been depicted in Fig 6. In this work, comparative results are shown for BER as key performance indicator.

4.1 Transmitter Block

Let the number of information bits be A. Initially CRC encoding is performed for error detection. Based on the desired output code rate R and code word length E, a polar code of length N (N=2n) is designed. The function of the rate matcher is to adjust the code length to match the available radio resources. Basic polar encoding is performed in the encoding kernel for a given code with N and a chosen information set. This polar encoded data is divided into sub-bands using serial to parallel converter. The parallel data streams are fed to the F-OFDM and UFMC transmitter block separately for waveform generation. Data is transmitted after UFMC or F-OFDM modulation via an array of NT transmitting antennas. Equation (10) shows the received vector NR×NT at the gNB.

$$Y=HX+\eta \tag{10}$$

where X denotes the transmitted signal, Y denotes the received signal and η is the complex Gaussian vector of white noise with zero mean. The channel matrix $H \in N_R \times N_T$ is deterministic and assumed to be always constant and known to both the transmitter and the receiver.

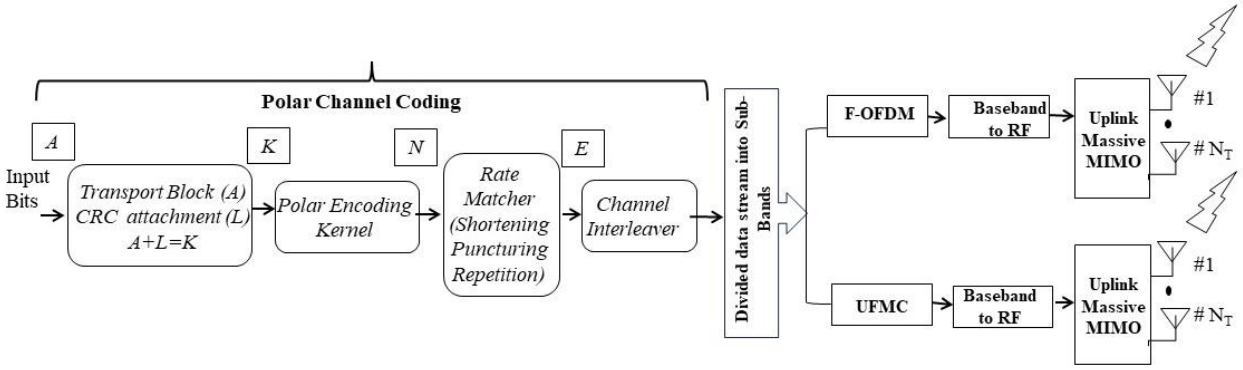

Fig. 6 Transmitter Block designed for simulation.

4.2 Receiver Block

The complete processing at the transmitting end and receiver end are presented in the form of flow chart shown in Fig. 7. At transmitting end data stream is generated, parameters are defined, pre-processed, channel coded, modulated, and finally transmitted.

At receiver end, the desired signal is detected by nullifying all the interference signals. It is done by inverting the effect of the channel by multiplying a suitable weight matrix W. In the system Zero forcing is used to detect the signal. In Zero forcing signal detection the interferences are nullified by weight matrix W_{ZF} represented in equation (11), called the Moore-Penrose pseudo-inverse of H [32].

$$W_{ZF}=(H^H H)^{-1}H^H \tag{11}$$

It inverts the effect of the channel and gives the expected value $\hat{x}_{ZF}$ by equation (12)

$$\hat{x}_{ZF}=\mathrm{S}\ \{(H^H H)^{-1}H^H\}Y \tag{12}$$

After the RF-link section the signal will pass through the time domain pre-processing window to suppress interference. Channel decoding is done for recovering the encoded input data stream, and here the Successive Cancellation List (SCL) algorithm implemented to get the original transmitted bits.

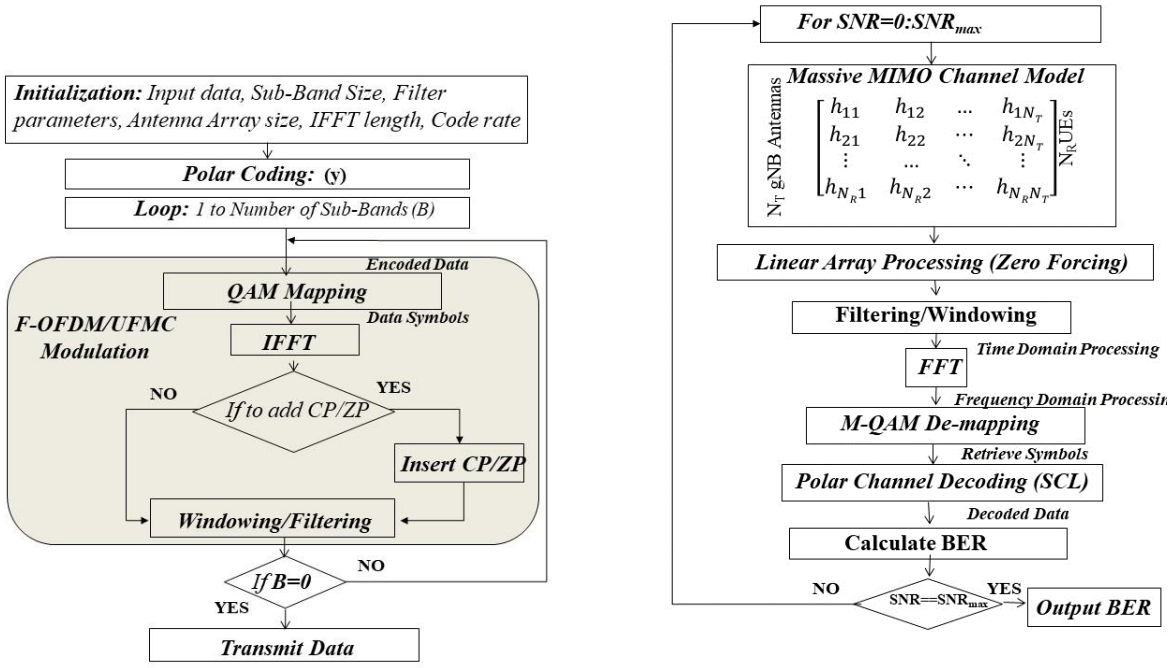

(a) (b)

Fig. 7 (a) Transmit end processing (b) Receiver end processing

5 Simulation and Results

The system is designed with 5G NR specifications based polar codes with F-OFDM and UFMC in massive MIMO scenario. For comparative analysis of both the waveforms the overall system uses Third Generation Partnership Project (3GPP) channel models under a 5G NR framework. The simulation is done using MATLAB software version 2022b. The simulation parameters are specified in Table 1.

Table 1 Simulation Parameters.

Parameter	Value
Common Waveform Parameters	
Number of Sub-bands (B)	10
Number of sub carriers in each Sub-band	20
Modulation order	64, 256 QAM
Size of FFT	512
F-OFDM Parameters	
Filter	Sinc with Hanning window
Filter Length	513
CP length	32
Tone offset	2.5
UFMC Parameters	
Filter	Dolph-Chebyshev
Filter Length	43
Sub-band Offset (O)	156
Side lobe attenuation (α)	40dB
Massive MIMO channel Parameters	
Number of Transmitting Antenna (N_T)	16
Number of Receiving Antenna at gNB (N_R)	20
Polar Coding Parameters	
Decoding List length (L)	8
Code rate R	1/2
Message length K	132
Rate matched output length E	256

Firstly, the basic F-OFDM and UFMC waveform simulated to observe the PAPR and BER performance based on QAM order. Fig 8 shows the normalized spectrum or power spectral density (PSD) of the F-OFDM and UFMC system with 20 sub-carriers in each sub-band.

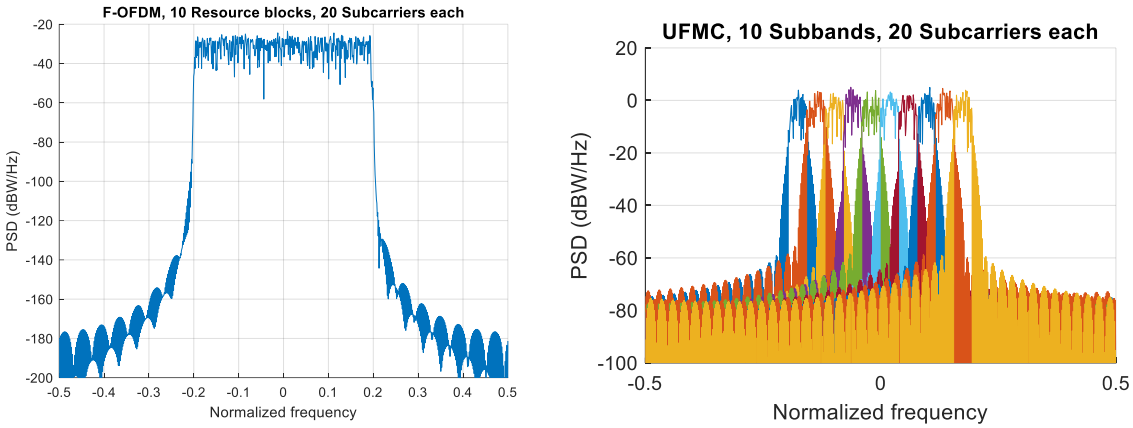

(a) (b)

Fig. 8 PSD with 200 Sub-carriers (a)F-OFDM (b)UFMC

From simulation results of Fig 9 obtained it is observed that as the QAM order increased, the BER performance degrades as expected due to increasing the bits per symbol. But comparing the BER for F-OFDM versus UFMC, it is concluded that F-OFDM achieves better BER than UFMC with SNR gain of approximately 5dB.As far as PAPR is measured, from Table II it is depicted that initially PAPR increases as QAM order is increased from 16QAM to 64QAM for both F-OFDM and UFMC technique. But for higher order QAM (256QAM or 1024QAM PAPR decreases). So, concluding that 256QAM or higher order supports high data rate as well as low PAPR at the compromise of BER performance. As can be seen from Table 2, that comparatively UFMC has lower PAPR than F-OFDM.

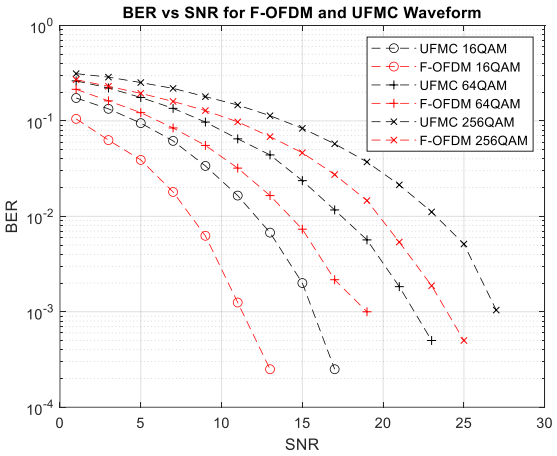

Fig. 9 BER Comparison for F-OFDM and UFMC for 64QAM and 256QAM

PC-UFMC waveform with SCL decoding is simulated in a massive MIMO scenario. F-OFDM and UFMC both use time-domain filtering with subtle differences in the way the filter is designed and applied. For UFMC, the length of filter is constrained to be equal to the cyclic-prefix length, while for F-OFDM, it can exceed the CP length [33]. The results for UFMC in massive MIMO are evaluated based on outcome mentioned in [34]. Fig 10 shows the BER performance of PC-UFMC for variable QAM order with 32x16 MIMO channel.

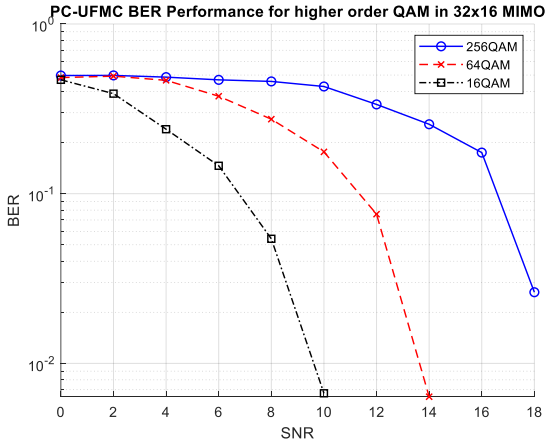

Fig. 10 BER Vs SNR for PC-UFMC in massive MIMO Rayleigh channel

PC-F-OFDM waveform is simulated in a massive MIMO scenario. Figure 10 (a) shows the BER performance of PC-F-OFDM with QPSK modulation in SISO and MIMO system and 10 (b) shows for variable QAM order with 32x16 MIMO channel. The results presented in [17] for polar coded F-OFDM system are compared with MIMO with similar simulation parameters in Fig 11 proving that MIMO enhances the BER performance by increasing the antenna array size. The simulation results shown in Fig 12 is generated in massive MIMO system with higher order QAM proved to be far

better than the results presented in [17] for polar coded F-OFDM system.

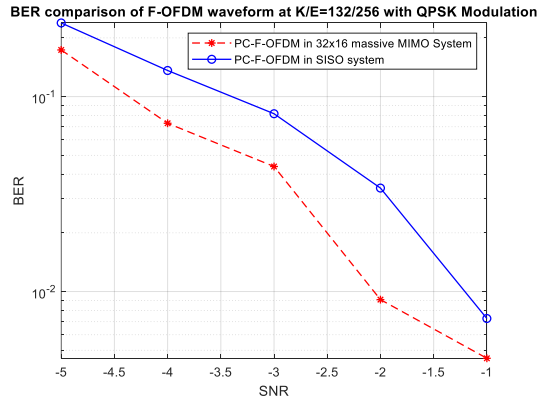

Fig. 11 BER Vs SNR for PC-F-OFDM With QPSK

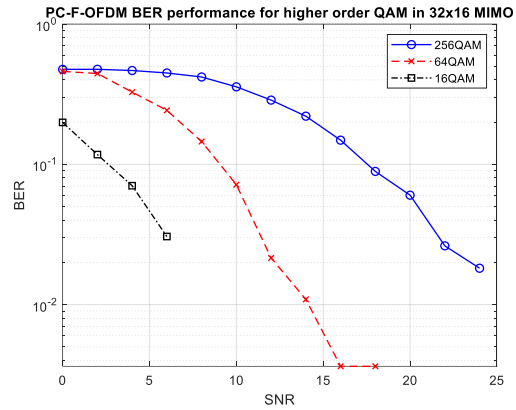

Fig. 12 BER Vs SNR for PC-F-OFDM higher order QAM in massive MIMO Rayleigh channel

Further, to observe the impact of distinct size of MIMO setup on the PC-F-OFDM and PC-UFMC waveform is simulated. Figures 13 and 14 show the BER performance for 256 and 64 QAM order with 32x16/64x16 MIMO channel.

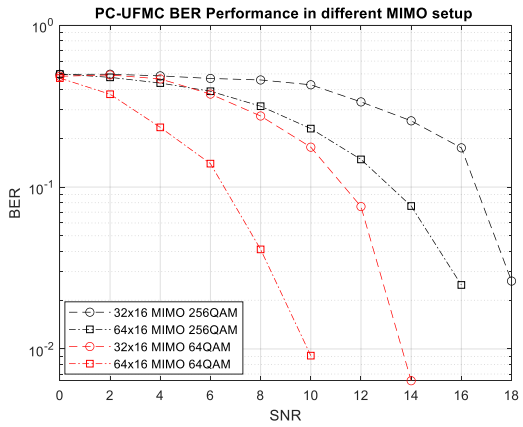

Fig. 13 BER performance of PC-UFMC in different MIMO setup

The results prove that the PC-UFMC waveform outperforms PC-F-OFDM in massive MIMO scenario. Although the PC-OFDM shows better performance than PC-UFMC in AWGN channel.

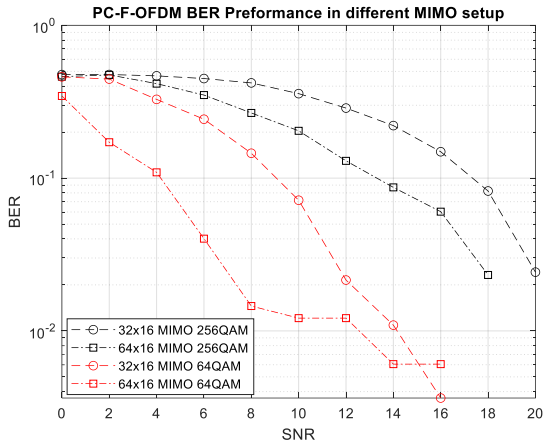

Fig. 14. BER performance of PC-F-OFDM in different MIMO setup

6 Conclusion

In this paper, an analytical framework for the polar coding with UFMC and f-OFDM modulation in massive MIMO scenario is designed. Under this framework, the BER performance at higher order QAM is proposed. Two different systems PC-UFMC and PC-F-OFDM are designed in 32x16 MIMO antenna setup to enhance the throughput and BER performance. Simulation results proved that the proposed PC-F-OFDM systems yield remarkably better performance compared with the PC-UFMC system. F-OFDM and UFMC are sub-band-wise filtered multicarrier waveform, but the filtering granularity is more flexible in f-OFDM than UFMC.

References

[1] ITU-R, “IMT Vision - Framework and overall objectives of the future development of IMT for 2020 and beyond,” Technical Report M.2083-0, Sept. 2015.

[2] Zhang, X. *et al.* (2016) ‘On the waveform for 5G’, *IEEE Communications Magazine*, 54(11), pp. 74–80. doi:10.1109/mcom.2016.1600337cm

[3] Qualcomm Inc., “Waveform candidates,” 3GPP Standard Contribution (R1-162199), Busan, Korea, Apr. 11-15, 2016.

[4] T. Hwang, C. Yang, G. Wu, S. Li, and G. Ye Li, "OFDM and Its Wireless Applications: A Survey," in IEEE Transactions on Vehicular Technology, vol. 58, no. 4, pp. 1673-1694, May 2009, doi: 10.1109/TVT.2008.2004555.

[5] R. Nissel, S. Schwarz, and M. Rupp, "Filter Bank Multicarrier Modulation Schemes for Future Mobile Communications," in IEEE Journal on Selected Areas in Communications, vol. 35, no. 8, pp. 1768-1782, Aug. 2017, doi: 10.1109/JSAC.2017.2710022.

[6] G. Fettweis, M. Krondorf and S. Bittner, "GFDM - Generalized Frequency Division Multiplexing," VTC Spring 2009 - IEEE 69th Vehicular Technology Conference, Barcelona, Spain, 2009, pp. 1-4, doi: 10.1109/VETECS.2009.5073571.

[7] F. Schaich, T. Wild and Y. Chen, "Waveform Contenders for 5G - Suitability for Short Packet and Low Latency Transmissions," 2014 IEEE 79th Vehicular Technology Conference (VTC Spring), Seoul, Korea (South), 2014, pp. 1-5, doi: 10.1109/VTCSpring.2014.7023145.

[8] X. Zhang, M. Jia, L. Chen, J. Ma, and J. Qiu, "Filtered-OFDM - Enabler for Flexible Waveform in the 5th Generation Cellular Networks," 2015 IEEE Global Communications Conference (GLOBECOM), San Diego, CA, USA, 2015, pp. 1-6, doi: 10.1109/GLOCOM.2015.7417854.

[9] Demir, Ali Fatih, Mohamed Elkourdi, Mostafa Ibrahim and Hüseyin Arslan. "Waveform Design for 5G and Beyond." 5G Networks: Fundamental Requirements, Enabling Technologies, and Operations Management (2018): n. pag.

[10] A. Hammoodi, L. Audah and M. A. Taher, "Green Coexistence for 5G Waveform Candidates: A Review," in IEEE Access, vol. 7, pp. 10103-10126, 2019, doi: 10.1109/ACCESS.2019.2891312.

[11] Van Eeckhaute, M., Bourdoux, A., De ncker, P. et al. Performance of emerging multi-carrier waveforms for 5G asynchronous communications. J Wireless Com Network 2017, 29 (2017). https://doi.org/10.1186/s13638-017-0812-8

[12] Y. Liu et al., "Waveform Design for 5G Networks: Analysis and Comparison," in IEEE Access, vol. 5, pp. 19282-19292, 2017, doi: 10.1109/ACCESS.2017.2664980.

[13] "3GPP TR 38.912 v15.0.0 Study on New Radio (NR) access technology (Release 15)".

[14] D. Hui, S. Sandberg, Y. Blankenship, M. Andersson, and L. Grosjean, "Channel Coding in 5G New Radio: A Tutorial Overview and Performance Comparison with 4G LTE," in IEEE Vehicular Technology Magazine, vol. 13, no. 4, pp. 60-69, Dec. 2018, doi: 10.1109/MVT.2018.2867640.

[15] Bae, Jung Hyun, Ahmed Attia Abotabl, Hsien-Ping Lin, Kee-Bong Song and Jungwon Lee. "An overview of channel coding for 5G NR cellular communications." APSIPA Transactions on Signal and Information Processing 8 (2019): n. pag. http://dx.doi.org/10.1017/ATSIP.2019.10

[16] Sharma, A., & Salim, M. (2019). Polar Code Appropriateness for Ultra-Reliable and Low-Latency Use Cases of 5G Systems. International Journal of Networked and Distributed Computing, 7(3), 93. https://doi.org/10.2991/ijndc.k.190702.005

[17] Deepa, T., Bharathiraja, N. Performance Evaluation of Polar Coded Filtered OFDM for Low Latency Wireless Communications. Wireless Pers Commun 116, 2023–2034 (2021). https://doi.org/10.1007/s11277-020-07777-2

[18] F. W. Vook, W. J. Hillery, E. Visotsky, J. Tan, X. Shao, and M. Enescu, ''System level performance characteristics of sub-6 GHz massive MIMO deployments with the 3GPP new radio,'' in Proc. IEEE VTC-Fall, Aug. 2018, pp. 1–5

[19] Chataut R, Akl R. Massive MIMO Systems for 5G and beyond Networks—Overview, Recent Trends, Challenges, and Future Research Direction. Sensors. 2020; 20(10):2753. https://doi.org/10.3390/s20102753

[20] Marzetta, T. L. (2010). Noncooperative Cellular Wireless with Unlimited Numbers of Base Station Antennas. IEEE Transactions on Wireless Communications, 9(11), 3590–3600. https://doi.org/10.1109/twc.2010.092810.091092

[21] J. Abdoli, M. Jia and J. Ma, "Filtered OFDM: A new waveform for future wireless systems," 2015 IEEE 16th International Workshop on Signal Processing Advances in Wireless Communications (SPAWC), Stockholm, Sweden, 2015, pp. 66-70, doi: 10.1109/SPAWC.2015.7227001.

[22] Ramadhan, Ali. (2022). Overview and Comparison of Candidate 5G Waveforms: FBMC, UFMC, and F-OFDM. International Journal of Computer Network and Information Security. 14. 27-38. 10.5815/ijcnis.2022.02.03.

[23] Zhang, Lei & Ijaz, Ayesha & Xiao, Pei & M. Molu, Mehdi & Tafazolli, Rahim. (2017). Filtered OFDM Systems, Algorithms and Performance Analysis for 5G and beyond. IEEE Transactions on Communications. PP. 10.1109/TCOMM.2017.2771242.

[24] H. Huawei, "F-OFDM scheme and filter design," in Proceedings of the 3GPP TSG RAN WG1 Meeting, vol. 85, pp. R1-165425), 2016.

[25] 3GPP. TSG RAN WG1 Meeting #85 R1-165425. f-OFDM Scheme and Filter Design. Available online: https://www.3gpp.org/DynaReport/TDocExMtg--R1-85--31662.htm

[26] Sakkas, L.; Stergiou, E.; Tsoumanis, G.; Angelis, C.T. "5G UFMC Scheme Performance with Different Numerologies" Electronics 2021, 10, 1915.

[27] Kishore, K. & Umar, P. & Jagan, Naveen. (2017). Comprehensive Analysis of UFMC with OFDM and FBMC. Indian Journal of Science and Technology. 10. 1-7. 10.17485/ijst/2017/v10i17/114337.
[28] Bioglio, Valerio et al. "Design of Polar Codes in 5G New Radio." IEEE Communications Surveys & Tutorials 23 (2018): 29-40.
[29] E. Arikan. Channel polarization: A method for constructing capacity-achieving codes for symmetric binary-input memoryless channels. IEEE Transactions on Information Theory, 55(7):3051–3073, July 2009. ISSN 0018-9448. doi:10.1109/TIT.2009.2021379.
[30] I. Tal and A. Vardy, "List decoding of polar codes," IEEE Transactions on Information Theory, vol. 61, no. 5, pp. 2213–2226, May 2015.
[31] Niu, Kai, and Kai Chen. "CRC-Aided Decoding of Polar Codes." IEEE Communications Letters, vol. 16, no. 10, Oct. 2012, pp. 1668–71. Crossref, https://doi.org/10.1109/lcomm.2012.090312.121501
[32] S. Yang and L. Hanzo, "Fifty Years of MIMO Detection: The Road to Large-Scale MIMOs," in IEEE Communications Surveys & Tutorials, vol. 17, no. 4, pp. 1941-1988, Fourthquarter 2015, doi: 10.1109/COMST.2015.2475242. https://in.mathworks.com/help/comm/ug/f-ofdm-vs-ofdm-modulation.html
[33] Deka, Surajit & Sarma, Kandarpa. (2020). JSCC-UFMC and Large MIMO Technology for High Data Rate Wireless Communication. International Journal of Mobile Computing and Multimedia Communications. 11. 10.4018/IJMCMC.2020100103.

Smita Jolania (Member, IEEE), holds a Bachelor of Engineering (Hons.) in Electronics and Communication, and a Master of Technology in Digital Communication. Currently, she is a Research Scholar at the Institute of Engineering and Technology, DAVV, in the domain of Wireless Communication Networks, 5G and beyond Networks and Signal Processing. She has published various research papers on the wireless cellular network in International Journals and conferences.

Dr. Ravi Sindal, Professor, Department of Electronics and Communication, IET, DAVV, received the B.E (Hons) degree from Rajasthan University, Jaipur in 1998. He received the M. Tech. Degree in Instrumentation and Ph.D. degree in Electronics and Telecommunication from Devi Ahilya University in 2000 and 2011, respectively. Since 2013, he has been a Professor of Electronics and Telecommunication at Institute of Engineering and Technology, Devi Ahilya University Indore. His research interests include Radio resource Management, Modeling and Simulation, Digital Design, and wireless networks. He has served on the program committee of various conferences. He has published many papers in various reputed International Journals and Conferences.